A Patient-Mounted Robotic Platform for CT-Scan Guided Procedures

Benjamin Maurin, *Member, IEEE*, Bernard Bayle*, Olivier Piccin, Jacques Gangloff, *Member, IEEE*, Michel de Mathelin, *Senior Member, IEEE*, Christophe Doignon, *Member, IEEE*, Philippe Zanne, and Afshin Gangi

***Abstract*—In this paper, we present a novel robotic assistant dedicated to medical interventions under computed tomography scan guidance. This compact and lightweight patient-mounted robot is designed so as to fulfill the requirements of most interventional radiology procedures. It is built from an original 5 DOF parallel structure with a semispherical workspace, particularly well suited to CT-scan interventional procedures. The specifications, the design, and the choice of compatible technological solutions are detailed. A preclinical evaluation is presented, with the registration of the robot in the CT-scan.**

***Index Terms*—Interventional radiology, medical robotics.**

I. Introduction

MEDICAL robotics applications recently opened a new field of investigation in robotic manipulation. Whereas first-generation medical robots were mostly industrial robots adapted to the medical field, new-generation systems are dedicated mechatronic devices. These systems are like smart surgical instruments able to perform a particular medical task with some guidance and with a noticeable improvement with respect to the manual procedure. Though these systems can still be considered as robots, they are completely different from standard industrial manipulators. Actually, they are characterized by compactness, lightness, good force/weight ratio, safety, and sterilizability. Design, driving, planning, and control problems resulting from these constraints can be considered as original and generic. In this paper, these robotic issues are analyzed through the development of a robotic platform compatible with computed tomography (CT) imaging.

Major breakthroughs in medical robotics have been achieved by robotic systems that use medical imaging to execute a given task [1]. CT-scan imaging is commonly used for manual percutaneous procedures, in the context of interventional radiology, for the treatment of chest or abdominal diseases [2]. Such minimally invasive treatments are less painful than open surgery and have many benefits: shorter operation duration, access to almost any organ, reduced trauma for the patient. These procedures consist in inserting a needle into the body of a patient in order to reach a target organ. Thanks to the CT-scan guidance, the radiologist can track the needle tip position. The major drawbacks of these procedures are the risk for the radiologist of excessive exposure to X-rays radiations and the lack of an accurate and real-time guidance system.

The concept of CT or MRI-guided needle insertions is not new. To our knowledge, Kwoh *et al.* [3] initiated the first work on stereotactic CT-scan guided surgery. Since then, the PAKY-RCM system [4], [5], initially devoted to kidney interventions, proved its efficiency in the operating room [6]. Computer-aided needle insertions were also used in clinical cases in other domains than abdominal surgery, e.g., neurosurgery [7] and with other imaging modalities, like ultrasound [8] or MRI [9]–[11]. Usually, robotic arms dedicated to interventional radiology are designed for safety reasons as reconfigurable passive guides. Systems such as the RoboPoint [12] or the B-Rob I [13] use active joints to position the instrument, but the insertion is performed manually by the physician. This approach, also found in commercial products like the Armstrong Pathfinder or the Innomotion [14], gives accurate results [15].

Still, a major difficulty in percutaneous treatments is due to the fact that the abdominal region moves with respect to the operation table when the patient breathes or accidentally coughs. The concept of a robotic system put on the patient's body has been proposed in [8], [16]–[20], as a passive and simple solution to physiological motion compensation. In fact, such a system does not actively compensate for breathing motions. However, as it moves with the patient body, breathing motions are no longer a problem. But, since the internal organs are usually moving in a quite different way, the compensation is only partial. There are two possible ways to overcome this problem: 1) the physiological motion of the target organ is compensated with an active method and 2) the needle is inserted and released during apnea phases. The first approach could be implemented with a visual servoing scheme requiring the scanner to be switched to the fluoroscopic mode. Yet, radiologists generally consider that long radiation exposures in fluoroscopic mode have to be avoided as much as possible. Therefore, in the approach presented in this paper, it is assumed that the needle is inserted during an apnea phase and then released.

Another major difficulty is to cope with the strict medical constraints of the needle insertion procedure: patient safety, CT-scan compatibility, sterilizability, compactness, lightness, full positioning, and orientation of the needle in space, registration.

Manuscript received April 20, 2007; revised November 27, 2007. First published June 10, 2008; current version published September 26, 2008. *Asterisk indicates corresponding author.*

B. Maurin, O. Piccin, J. Gangloff, M. de Mathelin, C. Doignon, and P. Zanne are with the Laboratoire des Sciences de l'Image, de l'Informatique et de la Télédétection (LSIIT), University of Strasbourg, National Center for Scientific Research (CNRS), France.

*B. Bayle is with the Laboratoire des Sciences de l'Image, de l'Informatique et de la Télédétection (LSIIT), University of Strasbourg, National Center for Scientific Research (CNRS), France.

A. Gangi is with the Department of Radiology B, University Hospitals of Strasbourg, France.

Color versions of one or more of the figures in this paper are available online at http://ieeexplore.ieee.org.

Digital Object Identifier 10.1109/TBME.2008.919882

TABLE I
CT-BOT SPECIFICATIONS

Features	Constraints	Solution
Safety	Motion compensation	Patient-mounted robot.
	Failsafe behavior	Quick removal of the robot from its base. Joints locked in case of power failure. Release of the needle.
Environmental compatibility	CT-scan compatibility	No metal in the CT-plane to avoid image artifacts.
	Sterilization	Protective bags, autoclavable distal parts, and one use parts.
Mechanical features	Dimensions	$\simeq$ 200 mm side cube (remaining space in the scanner ring for a stout patient).
	Weight	$<$ 3 kg for the patient comfort.
	Mobility	5 DOF according to physicians requirements; optional DOF for the needle self rotation (trajectory bending).
	Angular limits	-10 to 65 deg in the CT-plane, ± 25 deg in the orthogonal plane, to give access to various organs under various incidences.
	Accuracy	5 mm max position error at the tip of a 200 mm long needle ($\simeq$ 10 mm for a manual procedure).
	Forces	20 N max. force along the axis of the needle (see [23] for *in vivo* assessments of needle insertion forces).

To our knowledge, no patient-mounted platform has yet been designed in order to fulfill all these requirements. This is the contribution of the presented system, which is called CT-Bot. The outline of the paper follows the design procedure. Section II presents the specifications. The patient-mounted structure is derived from a task point of view and the prototype is presented in Section III. Section IV develops the technological issues. The registration of the robotic system is explained in Section V. Section VI consists of three experimental assessments of the CT-Bot. Finally, the CT-Bot key features are summarized, and possible further developments are discussed.

II. SYSTEM SPECIFICATIONS

The development of a robotic system for the operating room is dependent on several constraints. As detailed in [21], no particular methodology is needed to build a safe device, since no methodology will render safe an inherently unsafe device. However, engineers must make safety their top priority. A good summary of engineering guidelines for safe mechanical, electrical, or computer software design is proposed in [22]. Of course, in this paper, we set safety and CT-scan compatibility as the top priority goals. Additionally, we stated a list of specifications that meet the demanding requirements of interventional radiology procedures. Table I summarizes these specifications, each being the result of a given constraint.

III. DESIGN

A. Kinematics

From a kinematic viewpoint, the typical task to be achieved by the robotic assistant is to position and rotate a line supporting the principal axis of a surgical instrument such as a needle. Therefore, this specification can be fulfilled by a 5 DOF mechanical structure. Current solutions do not meet the required rigidity, orientation range, and compactness specifications. Parallel structures are rigid, compact, and characterized by a good absolute accuracy. However, they have a restricted workspace and a limited orientation range. On the other hand, serial manipulators exhibit a larger workspace, but are not compact and less rigid. Finally, parallel mechanisms are a better compromise to meet the specifications presented in Section II. Indeed, the system has to be built with some nonmetallic materials to avoid image artifacts. This yields greater flexibility in some linkages. So, any serial nonmetallic structure that we considered appeared neither compact, nor rigid enough to comply with the specifications. Since existing parallel structures do not fulfill all the requirements either, a specific design has been made to obtain a compact parallel structure with a larger than usual accessible workspace and with a wide orientation range.

The number of parallel mechanisms with 5 DOF is fairly small. Existing methods for the synthesis of such lower mobility (i.e., with less than 6 DOF) parallel mechanisms have only been used to find structurally symmetric parallel manipulators [24], [25], which do not fit our application, especially regarding the orientation range. Also, existing solutions often exhibit one or several central legs, which leave no room for a needle driving device. Finally, the topology synthesis of parallel manipulators cannot be disconnected from the dimensional synthesis problem. Therefore, we were brought to use simple planar and spatial linkages to form a novel architecture maximizing the orientation range.

The proposed robotic system is a parallel structure made of a six-bar linkage associated to a four-bar linkage joined together by a common platform, as pictured in Fig. 1.

The mechanism has 5 DOF: 3 DOF for the position and 2 DOF for the orientation. Three DOFs are imposed by the three actuators of the six-bar linkage. The second linkage constrains the remaining DOF of the first linkage thanks to two other actuators. It results in a 2R3T parallel manipulator driven by five actuators. The choice for the position of the motors results from a tradeoff. Putting motors on the joints connected to the base is not practical and may create collisions. Among the remaining possibilities, the motors were placed as near as possible to the base.

B. Modeling

This system has the noticeable property of having a complete set of analytical kinematic models, which is not generally the case for parallel mechanisms. The computation of the different models will not be developed in this paper, but further details can be found in [26]. To summarize, it turns out that multiple analytic solutions exist, either for the inverse kinematics (height

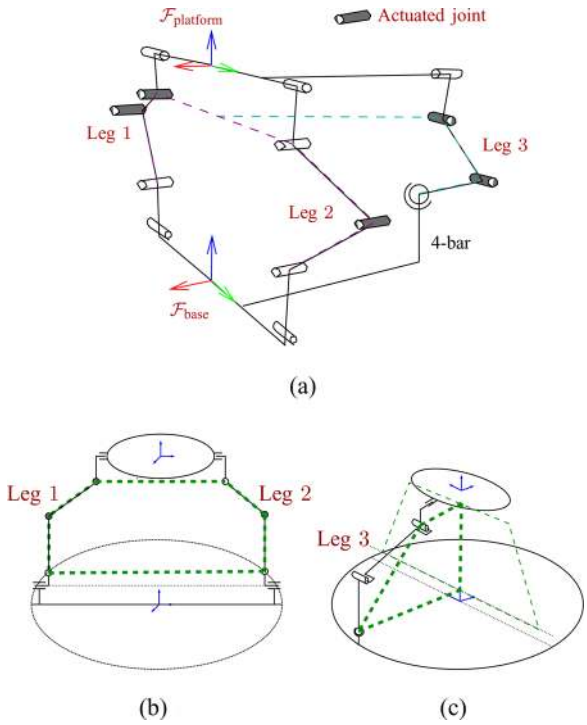

Fig. 1. (a) Kinematic structure of the system. (b) Six-bar linkage, legs 1 and 2. (c) Four-bar linkage, leg 3.

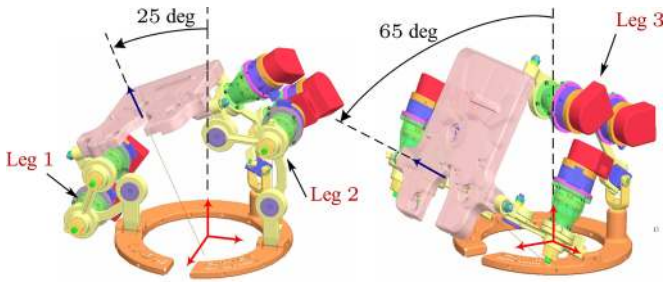

Fig. 2. Orientation range.

solutions) or for the forward kinematics (four solutions). The Jacobian matrix can also be calculated, either numerically using the first-order derivatives of the kinematics or analytically, which is more interesting for the analysis of singularities.

C. Prototype

From the proposed kinematic architecture, a physical system was designed. The lengths of the platform legs were optimized during the computer-aided design (CAD) procedure in order to avoid self-collisions as much as possible. It is also important to notice the particular arrangement of the legs that allows an easy access to the needle and to the workspace, for instance, to reach the intervention zone. The use of revolute joints rather than linear prismatic joints, together with an adequate choice of the legs length, allowed to build a compact platform with the adequate orientation range, as illustrated in Fig. 2.

The prototype, represented in Fig. 3, weights less than 2.5 kg. Most of the parts are made of resin or polymeric powder

Fig. 3. CT-Bot prototype with a passive needle guide.

and have been obtained through rapid prototyping with a laser sintering system or by stereolithography. However, the parts that guarantee the system rigidity, particularly the robot links, are made of metal (these parts do not cross the CT-scan plane).

Some improvements have been made at the interface between the body and the robot base. First, a robot base support is attached with straps on the patient body. To maximize the contact surface between the robot and the patient, a special interface was designed using a vacuum mattress. This mattress is filled with tiny polystyrene balls and it can be shaped accordingly to the surface of the patient's body. When the air is pumped out, the mattress becomes rigid and so ensures an optimal contact between the skin and the base of the robot. Furthermore, the robot first body has an open ring shape that matches the complementary shape of the base, so that the robot can be mounted on the base at different angular positions. This allows: 1) to choose the system initial orientation, for instance, to adapt the initial positioning to the workspace of the robot and 2) to remove or place the robot very quickly without having to unstrap the base from the patient.

IV. Driving, Control, and Planning

A. Driving System

1) Motors: Remember that a maximum force of 20 N might be required for a wide range of percutaneous interventions. As torques applied to the different joints depend on the exerted force and on the robot configuration, the corresponding maximum torque had to be determined, over the whole workspace. From the robot Jacobian, it comes that the maximum required torque for the most constrained joint is 2.5 N·m [27].

To comply with the specifications of safety, compactness, and lightness, ultrasonic actuators were preferred. In addition to their small size and high torque/weight ratio, ultrasonic motors are characterized by a good magnetic compatibility, a very fast response time, and also by a high holding torque that meets our safety constraints: when powered off, the holding torque is equal to the maximum torque. We chose the commercial Shinsei USR-30 rotary type ultrasonic motors.

2) Gearbox: To obtain the required torques, the motors are associated to 1/50 compact and backlash-free harmonic drive

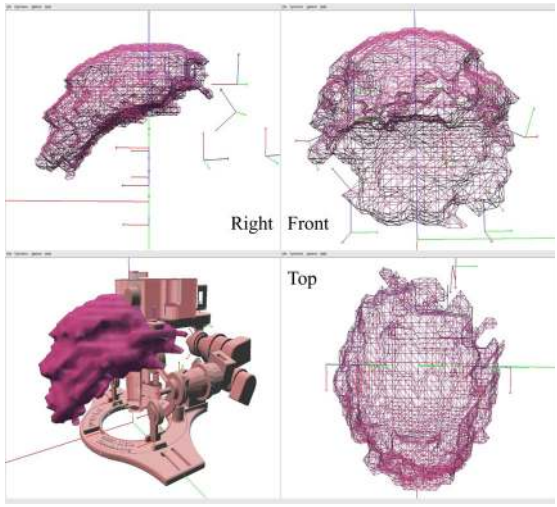

Fig. 4. Reachable workspace of the platform origin.

gears. Thus, the 0.05 N·m nominal torque of the Shinsei USR-30 is converted to a 2.5 N·m torque at the output shaft. The output shaft speed ranges from 0.063 to 0.586 rad/s, which is quite sufficient for the application. With its specific housing, each joint transmission fits in a $50\,\mathrm{mm} \times 30\,\mathrm{mm} \times 40$ mm box, which is very compact compared to other actuation technologies with the same torque range.

3) Control: Ultrasonic motors are connected to a power amplifier for the control of their angular velocity with an analog input. The velocity response of the motor with respect to this control signal is nonlinear, mainly because of a dead zone. Indeed, the velocity of the motor cannot go under a minimum value, which is 3.1 rad/s for the Shinsei USR-30 (only 0.063 rad/s at the gearbox output). This means that, for very slow motions, the motors work in a stepping mode. The digital joint position control loop of each motor uses the angular measurement feedback from an incremental encoder coupled to the motor shaft. A high proportional gain is sufficient to tune the position feedback loop, given the limited required dynamics. Indeed, since the motor dynamics is exceptionally fast and with no oscillatory modes, it is possible to achieve a very good rise time with no overshoot and almost no error, in spite of the dead zone.

B. Workspace and Planning

CAD volumes were converted into polyhedral representations, in order to compute the reachable workspace of the system. Thanks to the Opcode collision checking library [28], we could build the robot workspace for a given sampling of the robot configuration space, in order to determine the free configuration space CS_{free}, i.e., the set of the system possible configurations in which no self-collision occurs. Fig. 4 represents the accessible workspace for the origin of the platform frame. It appears that CS_{free} is compact and does not exhibit isolated prohibited zones. Additional illustrations of the accessible, the dextrous, and the orientation constrained workspace of the CT-Bot can be found in [27].

As CS_{free} is not convex, a collision-free path has to be computed systematically in order to avoid selfcollisions. Since the CT-Bot is a positioning platform, the fundamental requirement is to be able to compute a collision-free path between two given configurations of CS_{free}. The initial configuration is the current configuration of the system, and the target configuration is the desired configuration of the platform. It is computed from the inverse kinematic model since the position and orientation of the platform are defined by the task. Of course, the nearest configuration is chosen from the set of solutions given by the inverse kinematic model.

Then, a probabilistic path planning algorithm is used. It is based on the construction of a probabilistic roadmap (PRM) that is a graph that captures the topology of CS_{free}. CT-Bot planning module implements the visibility-PRM method [29], which allows to notably increase the performances of the basic PRM algorithm. Once an initial collision-free path is obtained, an optimization phase can be applied to smooth the initial path. It typically consists in resampling and modifying the obtained path so as to avoid discontinuities in the planned path.

C. Real-Time Control and Supervision Software

The control architecture is composed of the following.

1) A control PC based on a real-time Linux operating system (RTAI). This PC, dedicated to the control of the motors, is equipped with DAC/ADC cards and counter interfaces. The control software is based on a generic open-source control software developed in our laboratory. At the lowest level, selfcollisions are continuously tested thanks to the prebuilt CS_{free} grid. In this way, selfcollision avoidance is not only planned but also redundantly checked.
2) A PC dedicated to the supervision of CT-scan guided interventions with the CT-Bot. This machine is used as a human–machine interface (HMI) to visualize the CT-scan images and to communicate with the control PC through a fast 9 Mb/s serial link. A DICOM[1] client is used in the same interface. It allows to simulate and visualize simultaneously CT-scan images [30], the robot configuration, and the planned path.

This decoupled architecture offers a good solution to the problem of X-rays exposure: while the robot and its control unit are in the CT-scan room, the medical staff can remotely supervise the intervention behind a transparent protective screen, as represented in Fig. 5.

V. Registration

The positioning of the CT-Bot is a three-stage procedure. First, the base is placed purposely on the patient with radiopaque markers that are visible in the CT-scan image (see Fig. 6, left). So, the approximative positioning of the system in the vicinity of the target zone is achieved. Then, the vacuum mattress is emptied in order to realize a comfortable and somewhat rigid connection between the robot base and the patient. Finally, the robot itself is

[1]DICOM is a standard for handling, storing, and transmitting images and patient data in medical imaging.

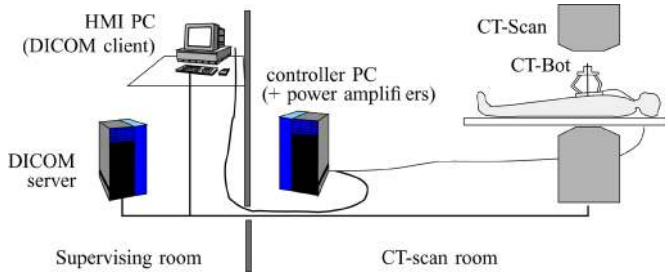

Fig. 5. Overall setup.

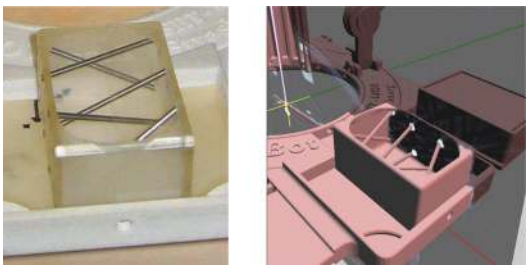

Fig. 6. Line fiducial object (left) and example of pose reconstruction visible in the HMI (right).

oriented and attached to the base support. This allows to choose the best initial configuration according to the intervention goal. Then, a registration of the robot has to be performed in order to calculate the homogeneous transformation between the two reference frames, respectively assigned to the CT-Bot and to the CT-scan. Finally, the configuration of the platform can be determined and the platform can be positioned and oriented, for a task specified in the CT-scan images. This is an important improvement over manual interventions.

To solve the registration problem, the existing approaches use CT-visible fiducial objects like a classical Brown–Roberts–Wells stereotactic frame [31], [32], or an external device like an optical tracker [33]. The stereotactic approaches allow to compute the pointing direction in the image when the robotic manipulator is properly registered, assuming that a perfect calibration of the robot and the needle relative to the CT-fiducials has been performed. The use of an external device requires to register the optical system with respect to the image frame and with respect to the needle driver, in order to achieve a correct image-guided procedure. To avoid the need of external fiducial objects and of external devices, we developed an original stereotactic registration method [34], using a random sample consensus approach combined to a numerical registration algorithm.

The robot registration proceeds as follows. A DICOM image is sent to the supervising computer and displayed in the graphical user interface. After a limited number of manipulations of the operator, the robot is automatically registered with respect to the image. Afterwards, the radiologist can plan its intervention directly in the image. An example of an automatic pose registration is presented in Fig. 6. The automatic registration of the fiducial pose is achieved and the error is estimated from a projection of the CT-scan image in the HMI of the robot. A pose registration error of less than 1 mm is measured from the reconstruction images. The robustness of the pose reconstruction algorithm has been validated through statistical tests.

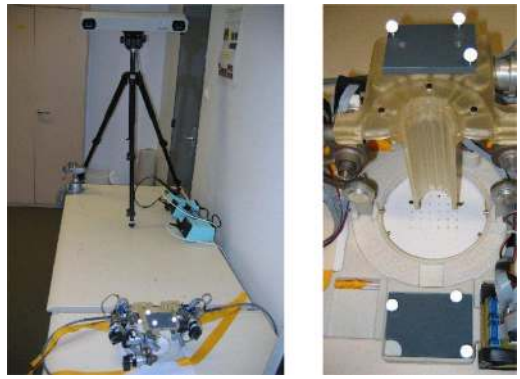

Fig. 7. End effector position given by a Polaris: experimental setup.

VI. Experiments

The following section presents an evaluation of the CT-Bot prototype through three different experiments. In the first one, the system is moved to successive poses and its mechanical accuracy is measured by an exteroceptive sensor. In the second and third experiments, the robot is placed on a phantom, in the CT-scan. It is registered, and its ability to point a target defined in the CT-scan image is then evaluated.

A. First Experiment

This experiment consists in different point-to-point motions. Each motion starts and ends at the initial configuration, and five other poses of the platform are specified to the robot controller. Finally, the robot position and orientation accuracy is evaluated in 30 successive configurations, among which ten are different.

The platform poses are measured with a Polaris to evaluate the absolute accuracy of the CT-Bot. The Polaris is an optical stereo tracking system [35] that allows to simultaneously localize several markers with a 0.35 mm accuracy. To perform this evaluation, two Polaris markers are placed, respectively, on the robot platform and on the robot base, as illustrated in Fig. 7. At the end of each point-to-point motion, the pose of the target placed on the platform is measured with respect to the base and compared to the desired pose.

The position and orientation errors are determined by calculating for each pose: 1) the distance between the reference position and the measured position and 2) the angle between the reference vector (perpendicular to the platform) and the measured one. An RMS value of 0.76 mm (respectively, 0.45°) is obtained for the position (respectively, orientation) error, with a standard deviation of 0.39 mm (respectively, 0.25°). Using the Student's *t*-distribution because of the limited number of measurement samples, we can estimate the confidence interval of the proposed results. The 95% confidence interval for the mean position (respectively, orientation) error is $[0.43; 1.09]$ mm (respectively, $[0.26; 0.66]^\circ$).

Since these results correspond to measurements at the platform level, they have to be completed by evaluations of the

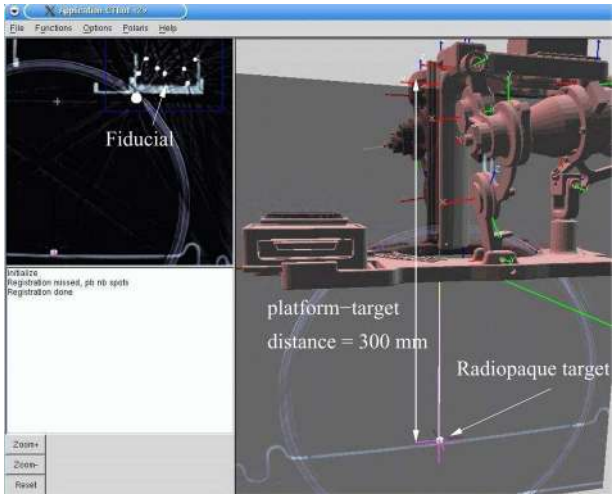

Fig. 8. Task path planning.

position error at the needle tip. The extrapolation of the position and angular errors at a distance of 300 mm gives[2] a mean position error of 2.79 mm. Finally, the system accuracy in laboratory conditions remains compatible with the specifications claimed in Section II. In the following two paragraphs, measurements at the needle tip are performed, with the robot registered in the CT-scanner, and it is shown that the accuracy of the registered system is also sufficient.

B. Second Experiment: Laser Pointing Task

This experiment is conducted to check the ability to position and rotate the system in order to point at a target defined in the CT-scan image. We place the target so that it can be reached with a laser source mounted on the platform at a distance of 300 mm from the target (see Fig. 8; note that the needle guide is not used in this case, though it appears on the virtual view of the HMI). The pointing accuracy is then checked visually, thanks to the laser beam projection.

First, a region of interest is specified for the segmentation of the fiducials. Then, the system is automatically registered thanks to the projection of the fiducial object in the DICOM image, as visible in Fig. 8. An average RMS registration error of 0.05 mm was obtained for each spot centroid location (0.09 pixel). Then, the HMI is used to define two points in the CT-scan image: the target point and a virtual entry point. The target point is materialized by a small 5×3 mm radiopaque sample, which can be visible in at least one CT-scan slice, as pictured in Fig. 8. Note that the distance between two successive CT-scan planes was 2 mm in this experiment.

Finally, the pointing accuracy is visually assessed thanks to the laser source mounted on the robot platform. With a worst-case estimation of the size of projection of the laser spot on the target, we could measure an average accuracy of less than 3 mm in the pointing task.

[2]Note that a 300 mm distance between the robot platform and the target is chosen voluntarily high to obtain a pessimistic evaluation.

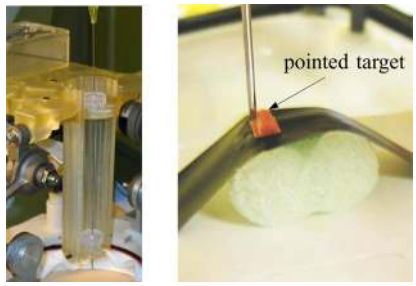

Fig. 9. Needle pointing task.

TABLE II
CT-BOT ACCURACY FOR THE THREE EXPERIMENTS

Exp.	Platform to target distance	Sensing resolution	Mean error	Upper bound error
1	300 mm	0.35 mm	2.79 mm	–
2	300 mm	1 mm	–	3 mm
3	200 mm	1.5 mm	–	5 mm

C. Third Experiment: Manual Needle Insertion

The method in this experiment is nearly the same as in the previous laser pointing task. We replace the laser device by a manual passive needle guide, as is visible in Figs. 3 and 9. A radiopaque marker is placed under the skin of an abdominal phantom and targeted using the HMI. An entry point on the phantom surface is chosen, thus defining the insertion direction. Once the system has been positioned in the corresponding pose, a 16-gauge, 200-mm-long biopsy needle is inserted after a small incision on the phantom artificial skin, as is usual in interventional radiology.

The needle is inserted until it reached the surface on which the target is attached, at a depth of 65 mm from the phantom skin surface. Then, the needle tip position error is measured, as illustrated in Fig. 9. During successive tests, we obtained a 5 mm accuracy in the worst case. Note that given the distance between the passive holder and the skin, the actual needle translation was 100 mm.

D. Discussion

The previous results, summarized in Table II, are compatible with our initial specifications.

These experiments underline different issues that act on the accuracy of the system. The first experiment allowed to evaluate its mechanical accuracy. Improvement of the mechanical accuracy could certainly be obtained using conventional manufacturing means instead of rapid prototyping. The second and the third experiments aim at measuring the system accuracy for a task defined in the CT-scan image. In this case, the result depends not only on the mechanical accuracy of the CT-Bot, but also on the registration of the system. In the second experiment, a long distance pointing is achieved. The comparison between the results obtained in experiments 1 and 2 shows that the error due to the registration procedure has a very limited effect on the system accuracy. In the third experiment, the insertion of a needle into an artificial phantom makes possible the evaluation

of the accuracy of a typical CT-scan intervention achieved in laboratory conditions. Note that the performed needle insertion experiment does not correspond to the full specifications, since an insertion shorter than 200 mm has been finally achieved. However, this experiment also proposed as a benchmark in [36] can be used in order to make a comparison with other patient-mounted systems. The initial objective of [36], which is to reach a 10 mm target, was achieved in a satisfactory manner for insertion distances lower than 30 mm. In our case, we could evaluate an insertion accuracy of less than 5 mm for 65-mm-long insertions through the skin. Therefore, the results proposed in this paper contribute to the improvement of body-mounted systems dedicated to CT-scan interventions.

VII. Conclusion

In this paper, we have presented the design and the implementation of a robot dedicated to CT-scan guided interventions. We selected a parallel structure mounted on the patient's abdomen to fit the medical specifications. We pointed out the various technological issues that had to be specifically taken into account to design the system: compactness, intrinsic safety, high forces, and high accuracy.

We evaluated the ability of the prototype to fulfill the accuracy requirements. Absolute positioning was evaluated using an external measurement system. The ability of the system to point a target under CT-scan guidance was also validated. An accuracy of less than 3 mm was observed with a laser pointing experiment, for a typical intervention depth. Finally, a manual needle insertion was performed and an accuracy of less than 5 mm was measured using a 200-mm-long needle. These performances match the initial specifications, with the limitation that they were obtained in laboratory circumstances.

Perspectives include the evaluation of this system in the context of *in vivo* needle insertion tasks. Then, the influence of the needle bending, which has not been treated in this paper, will have to be considered. In the perspective of automated or teleoperated needle insertions, the design and manufacturing of a dedicated needle driver will be another future direction of investigation.

References

[1] R. Taylor, "Medical robotics and computer-integrated therapy delivery: Coupling information to action in 21'st century therapeutic interventions," presented at the NSF Workshop Next Generation Human Assist Devices Autom. Med. Robot. Comput.-Integr. Surg., Baltimore, MD, 2000.

[2] J. A. Kaufman and M. J. Lee, *Vascular and Interventional Radiology—The Requesites*. Amsterdam, The Netherlands: Elsevier, 2004.

[3] Y. S. Kwoh, J. Hou, E. Jonckheere, and S. Hayati, "A robot with improved absolute positioning accuracy for CT guided stereotactic brain surgery," *IEEE Trans. Biomed. Eng.*, vol. 35, no. 2, pp. 153–160, Feb. 1988.

[4] D. Stoianovici, L. Whitcomb, J. Anderson, R. Taylor, and L. Kavoussi, "A modular surgical robotic system for image guided percutaneous procedures," in *Proc. Med. Image Comput. Comput.-Assisted Intervention*, Cambridge, MA, 1998, pp. 404–410.

[5] K. Masamune, G. Fichtinger, A. Patriciu, R. Susil, R. Taylor, L. Kavoussi, J. Anderson, I. Sakuma, T. Dohi, and D. Stoianovici, "System for robotically assisted percutaneous procedures with computer tomography guidance," *Comput. Aided Surg.*, vol. 6, pp. 370–383, 2001.

[6] L. Su, D. Stoianovici, T. Jarrett, A. Patriciu, W. Roberts, J. Cadeddu, S. Ramakumar, S. Solomon, and L. Kavoussi, "Robotic percutaneous access to the kidney: Comparison with standard manual access," *J. Endourol.*, vol. 7, no. 16, pp. 471–475, 2002.

[7] S. Lavallee, J. Troccaz, L. Gaborit, P. Cinquin, A. Benabid, and D. Hoffmann, "Image-Guided Operating Robot: A Clinical Application in Stereotactic Surgery," *Computer Integrated Surgery*, Cambridge, MA: MIT Press, 1995, pp. 343–352.

[8] J. Hong, T. Dohi, M. Hashizume, K. Konishi, and N. Hata, *An ultrasound-driven needle-insertion robot for percutaneous cholecystostomyPhysics in Medicine and Biology*. London, U.K.: IOP Publishing, 2004, pp. 441–455.

[9] H. Naganou, H. Iseki, and K. Masamune, "Mri-compatible modular designed robot for interventional navigation — prototype development and evaluation," in *Proc. Med. Image Comput. Comput.-Assisted Intervention*, Saint-Malo, France, 2004, pp. 1069–1070.

[10] A. Krieger, R. Susil, C. Ménard, J. Coleman, G. Fichtinger, E. Atalar, and L. Whitcomb, "Design of a novel MRI compatible manipulator for image guided prostate interventions," *IEEE Trans. Biomed. Eng.*, vol. 52, no. 2, pp. 306–313, Feb. 2005.

[11] M. Bock, A. Melzer, H. Bardenheuer, H. Ghaderi, B. Gutmann, H. Zimmermann, and W. Semmler, "MR-Guided percutaneous interventions using a robotic assistance system: Initial experiences in a pig model," in *Proc. Conf. Int. Soc. Magn. Resonance Med.*, Miami, FL, 2005, pp. 2665–2670.

[12] D. Schauer, A. Hein, and T. C. Lueth, "Robopoint. An autoclavable interactive miniature robot for surgery and interventional radiology," *Int. Congress Series*, vol. 1256, pp. 555–560, 2003.

[13] G. Kronreif, M. Fürst, J. Kettenbach, M. Figl, and R. Hanel, "Robotic guidance for percutaneous interventions," *Adv. Robot.*, vol. 17, no. 6, pp. 541–560, 2003.

[14] A. Melzer, B. Gutmann, A. Lukoschek, and M. Mark, "Experimental evaluation of an MRI compatible telerobotic system for CT MRI guided interventions," *Suppl. Radiol.*, vol. 44, p. 409, 2003.

[15] P. Morgan, A. Sepehri, J. Punt, P. Byrne, A. Moody, T. Carter, S. Davis, and P. Finlay, "The application accuracy of the pathfinder neurosurgical robot," presented at the Comput. Assisted Radiol. Surg. Conf., London, U.K., 2003.

[16] P. J. Berkelman, P. Cinquin, J. Troccaz, J.-M. Ayoubi, C. Létoublon, and F. Bouchard, "A compact, compliant laparoscopic endoscope manipulator," in *Proc. IEEE Int. Conf. Robot. Autom.*, Washington, DC, 2002, pp. 1870–1875.

[17] M. Shoham, M. Burman, E. Zehavi, L. Joskowicz, E. Batkilin, and Y. Kunicher, "Bone-mounted miniature robot for surgical procedures: Concept and clinical applications," *IEEE Trans. Robot. Autom.*, vol. 19, no. 5, pp. 893–901, Oct. 2003.

[18] A. Vilchis, J. Troccaz, P. Cinquin, K. Masuda, and F. Pelissier, "A new robot architecture for tele-echography," *IEEE Trans. Robot. Autom.*, vol. 19, no. 5, pp. 922–926, Oct. 2003.

[19] B. Maurin, O. Piccin, B. Bayle, J. Gangloff, M. de Mathelin, L. Soler, and A. Gangi, "A new robotic system for CT-guided percutaneous procedures with haptic feedback," presented at the Comput. Assisted Radiol. Surg. Conf., Chicago, IL, 2004.

[20] P. Berkelman, J. Troccaz, and P. Cinquin, "Body-supported medical robots: A survey," *J. Robot. Mechatron.*, vol. 16, no. 5, pp. 513–517, 2004.

[21] P. Varley, "Techniques for development of safety-related software for surgical robots," *IEEE Trans. Inform. Technol. Biomed.*, vol. 3, no. 4, pp. 261–267, Dec. 1999.

[22] A. Rovetta, "Telerobotic surgery control and safety," in *Proc. IEEE Int. Conf. Robot. Autom.*, San Francisco, CA, 2000, pp. 2895–2900.

[23] B. Maurin, L. Barbe, B. Bayle, P. Zanne, J. Gangloff, M. de Mathelin, A. Gangi, and A. Forgionne, "*In vivo* study of forces during needle insertions," presented at the Med. Robot., Navigat. Visualisation Sci. Workshop, Remagen, Germany, 2004.

[24] Q. Li, Z. Huang, and J. Hervé, "Type synthesis of 3R2T 5-DOF parallel mechanisms using the Lie group of displacements," *IEEE Trans. Robot. Autom.*, vol. 20, no. 3, pp. 173–180, Apr. 2004.

[25] X. Kong and C. Gosselin, "Type synthesis of 5-DOF parallel manipulators based on screw theory," *J. Robot. Syst.*, vol. 22, pp. 535–547, 2005.

[26] B. Maurin, O. Piccin, B. Bayle, J. Gangloff, and M. de Mathelin, "A parallel 5 DOF positioner for semi-spherical workspaces," presented at the ASME Design Eng. Tech. Conf., Salt Lake City, UT, 2004.

[27] B. Maurin, "Conception et réalisation d'un robot d'insertion d'aiguille pour les procédures percutanées sous imageur scanner," Ph.D. dissertation, Univ. Louis Pasteur, Strasbourg, France, 2005.

[28] P. Terdiman Opcode—OPtimized Collision DEtection. (2008). [Online]. Available: http://www.codercorner.com/Opcode.htm

[29] T. Siméon, J.-P. Laumond, and C. Nissoux, "Visibility based probabilistic roadmaps for motion planning," *Adv. Robot.*, vol. 14, no. 6, pp. 477–493, 2000.
[30] DCMTK-DICOM toolkit. (2008). [Online]. Available: http://www.dicom.offis.de
[31] R. C. Susil, J. H. Anderson, and R. H. Taylor, "A single image registration method for ct guided interventions," in *Proc. Med. Image Comput. Comput.-Assisted Intervention*, Cambridge, U.K., 1999, pp. 798–808.
[32] G. Fichtinger, T. L. DeWeese, A. Patriciu, A. Tanacs, D. Mazilu, J. H. Anderson, K. Masamume, R. H. Taylor, and D. Stoianovici, "Robotically assisted prostate biopsy and therapy with intra-operative CT guidance," *J. Acad. Radiol.*, vol. 9, pp. 60–74, 2002.
[33] K. Cleary, M. Freedman, M. Clifford, D. Lindisch, S. Onda, and L. Jiang, "Image-guided robotic delivery system for precise placement of therapeutic agents," *J. Controlled Release*, vol. 74, pp. 363–368, 2001.
[34] B. Maurin, C. Doignon, M. de Mathelin, and A. Gangi, "Pose reconstruction with an uncalibrated computed tomography imaging device," in *Proc. IEEE Int. Conf. Comput. Vision Pattern Recog.*, 2003, pp. 455–460.
[35] NDI polaris system. (2008). [Online]. Available: http://www.ndigital.com/polaris.php
[36] E. Taillant C., J.-C. Avila-Vilchis, I. Bricault, and P. Cinquin, "CT and MR compatible light puncture robot: Architectural design and first experiments," in *Proc. Med. Image Comput. Comput.-Assisted Intervention*, Saint-Malo, France, 2004, pp. 145–152.

Benjamin Maurin (S'01–M'05) received the Electr. Eng. degree from the Ecole Nationale Supérieure de Physique de Strasbourg (ENSPS), in 2001 and the Ph.D. degree in medical robotics and computer vision from the University Louis Pasteur, Strasbourg, France, in 2005.

Since 2006, he has been engaged as a Research and Development Engineer for Cerebellum Automation. His current research interests include motion control for high speed robotic systems and computer vision.

Bernard Bayle was born in 1972. He received the Electr. Eng. degree from the Ecole Normale Supérieure de Cachan, Cachan, France, in 1995, and the M.S. and Ph.D. degrees in robotics and control from the Laboratoire d'Architecture et d'Analyse des Systémes (LAAS), National Center for Scientific Research (CNRS), University of Toulouse, Toulouse, France, in 1996 and 2001, respectively.

Since 2002, he has been an Associate Professor at the Ecole Nationale Supérieure de Physique (ENSPS), University of Strasbourg, Strasbourg, France. His current research interests include robotic manipulation, medical robotics, haptics, and teleoperation.

Olivier Piccin received the Mech. Eng. degree from the Ecole Nationale Supérieure d'Arts et Métiers (ENSAM), Toulouse, France, and the Ph.D. degree from the Laboratoire d'Architecture et d'Analyse des Systémes (LAAS), National Center for Scientific Research (CNRS), University of Toulouse, Toulouse, in 1992 and 1995, respectively.

During 1996, he was the Head of the robotics and automation service for body-in-white spot welding applications in PSA-Peugeot Citroën Company, Vélizy, France. Since 1998, he has been an Associate Professor in the Department of Mechanical Engineering, National Institute of Applied Sciences (INSA), Strasbourg, France, where he is engaged in classical mechanics, mechanics for polyarticulated systems, and computer-based tools for mechanical engineering. His current research interests include medical robotics and mechanical design.

Dr. Piccin is a member of the American Society of Mechanical Engineers (ASME).

Jacques Gangloff (S'96–M'99) received the Electr. Eng. degree from the Ecole Nationale Supérieure de Cachan, Cachan, France, in 1995, and the M.S. and Ph.D. degrees in robotics from the University Louis Pasteur, Strasbourg, France, in 1996 and 1999, respectively.

From 1999 to 2005, he was an Associate Professor in the University of Strasbourg, Strasbourg, where since 2005, he has been a Professor. He is currently a member of the Control Vision and Robotics Team, Laboratoire des Sciences de l'Image, de l'Informatique et de la Télédétection (LSIIT), University of Strasbourg, Strasbourg. His current research interests include visual servoing, predictive control, and medical robotics.

Dr. Gangloff was the recipient of the Best Vision Paper Award at the IEEE International Conference on Robotics and Automation (ICRA) in 2004 and the 2005 Best Paper Award of the IEEE Transactions on Robotics and Automation.

Michel de Mathelin (SM'02) received the Electr. Eng. degree from Louvain University, Louvain-La-Neuve, Belgium, in 1987, and the M.S. and Ph.D. degrees in electrical and computer engineering from the Carnegie Mellon University, Pittsburgh, PA, in 1988 and 1993, respectively.

During 1991–1992, he was a Research Scientist in the Department of Electrical Engineering, Polytechnic School of the Royal Military Academy, Brussels, Belgium. In 1993, he was an Assistant Professor at Strasbourg University, France. Since 1999, he has been a Professor at the Ecole Nationale Supérieure de Physique de Strasbourg (ENSPS), Strasbourg, France. Since 2003, he has been an Associate Editor of the *IEEE Control System Technology Journal*. His current research interests include medical robotics, visual servoing, adaptive, and robust control.

Dr. Mathelin is a fellow of the Belgian American Educational Foundation.

Christophe Doignon (M'00–M'03) received the Electr. Eng. degree from the Ecole Nationale Supérieure de Physique de Strasbourg (ENSPS), Strasbourg, France, and the Ph.D. degree in computer vision and robotics from the University Louis Pasteur, Strasbourg, in 1989 and 1994, respectively, and the Habilitation diriger des Recherches (HDR) Diploma in the same University in 2007.

In 1995 and 1996, he was in the Department of Electronics and Computer Science, Padua University, Padua, Italy. Since 1996, he has been an Assistant Professor in computer engineering in the Control, Vision and Robotics Team, Laboratoire des Sciences de l'Image, de l'Informatique et de la Télédétection (LSIIT), National Center for Scientific Research (CNRS), University of Strasbourg, Strasbourg. His current research interests include computer vision, signal and image processing, visual servoing, and robotics.

Philippe Zanne received the Electr. Eng. degree from the Ecole Nationale Supérieure de Physique de Strasbourg, Strasbourg, France, in 1998, and the M.S. and Ph.D. degrees in robotics from the University Louis Pasteur, Strasbourg, France, in 1999 and 2003, respectively.

Since 2002, he has been a Research Engineer with the National Center for Scientific Research (CNRS), Strasbourg, where he is a member of the Control, Vision, and Robotics Team, Laboratoire des Sciences de l'Image, de l'Informatique et de la Télédétection (LSIIT). His current research interests include visual servoing, robust control, and medical robotics.

Afshin Gangi was born on December 7, 1962. He received the M.S. degree in medical biology from the University Claude-Bernard, Lyon, France, in 1994, and the Ph.D. degree in laser physics at the National Scientific Research Center (CNRS), University of Strasbourg, Strasbourg, France, in 1997.

During 1997, he was an Associate Professor in diagnostic and interventionnal radiology at the University Hospital of Strasbourg, Strasbourg, where since 2000, he has been a Full Professor of radiology, and he is currently the Head of the Radiological Department. He is also an Associated Professor at King's College of London, London, U.K. He is the author or coauthor of several papers published in journals and conferences in the field of nonvascular radiology.

Prof. Gangi was the recipient of the several awards at international meetings, particularly those focused on pain treatment under radiological guidance.